

## Article

# Serotonin-Derived Fluorophore: A Novel Fluorescent Biomaterial for Copper Detection in Urine

Mariagrazia Lettieri <sup>1</sup>, Simona Scarano <sup>1</sup>, Laura Caponi <sup>2</sup>, Andrea Bertolini <sup>3</sup>, Alessandro Saba <sup>2,3</sup>, Pasquale Palladino <sup>1,\*</sup> and Maria Minunni <sup>1,\*</sup>

<sup>1</sup> Department of Chemistry 'Ugo Schiff', University of Florence, 50019 Sesto Fiorentino, Italy

<sup>2</sup> Laboratory of Clinical Pathology, University Hospital of Pisa, 56126 Pisa, Italy

<sup>3</sup> Department of Surgical, Medical and Molecular Pathology and Critical Care Medicine, University of Pisa, 56126 Pisa, Italy

\* Correspondence: pasquale.palladino@unifi.it (P.P.); maria.minunni@unifi.it (M.M.)

**Abstract:** We took advantage of the fluorescent features of a serotonin-derived fluorophore to develop a simple and low-cost assay for copper in urine. The quenching-based fluorescence assay linearly responds within the concentration range of clinical interest in buffer and in artificial urine, showing very good reproducibility ( $CV_{av}\% = 4\%$  and  $3\%$ ) and low detection limits ( $16 \pm 1 \mu\text{g L}^{-1}$  and  $23 \pm 1 \mu\text{g L}^{-1}$ ). The  $\text{Cu}^{2+}$  content was also estimated in human urine samples, showing excellent analytical performances ( $CV_{av}\% = 1\%$ ), with a limit of detection of  $59 \pm 3 \mu\text{g L}^{-1}$  and a limit of quantification of  $97 \pm 11 \mu\text{g L}^{-1}$ , which are below the reference value for a pathological  $\text{Cu}^{2+}$  concentration. The assay was successfully validated through mass spectrometry measurements. To the best of our knowledge, this is the first example of copper ion detection exploiting the fluorescence quenching of a biopolymer, offering a potential diagnostic tool for copper-dependent diseases.

**Keywords:** serotonin; serotonin-derived fluorophore; urine analysis; fluorescence quenching; copper detection; copper-dependent diseases; copper poisoning



**Citation:** Lettieri, M.; Scarano, S.; Caponi, L.; Bertolini, A.; Saba, A.; Palladino, P.; Minunni, M.

Serotonin-Derived Fluorophore: A Novel Fluorescent Biomaterial for Copper Detection in Urine. *Sensors* **2023**, *23*, 3030. <https://doi.org/10.3390/s23063030>

Academic Editor: Maria Strianese

Received: 1 March 2023

Revised: 8 March 2023

Accepted: 9 March 2023

Published: 10 March 2023

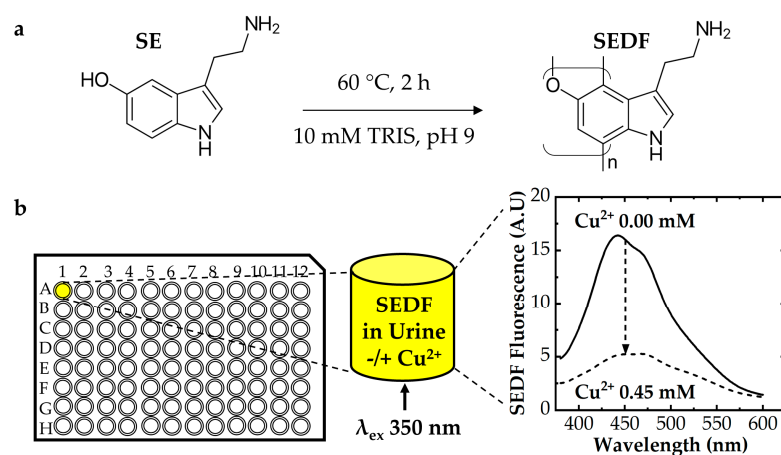


**Copyright:** © 2023 by the authors. Licensee MDPI, Basel, Switzerland. This article is an open access article distributed under the terms and conditions of the Creative Commons Attribution (CC BY) license (<https://creativecommons.org/licenses/by/4.0/>).

## 1. Introduction

Copper ion is essential to living systems, regulating many physiological functions, acting as a cofactor of numerous enzymes (e.g., dopamine  $\beta$ -hydroxylase, tyrosinase, and cytochrome c oxidase [1]), contributing to cellular and tissue growth, and working as an antioxidant [2]. The World Health Organization (WHO) recommends an intake of  $30 \mu\text{g}$  per kilogram of body weight per day [3]. However, an excess of this heavy metal leads to protein structure modification, interfering with the exchange of zinc in metalloproteins and compromising most cellular functions [4]. Recently, it was demonstrated that an accumulation of  $\text{Cu}^{2+}$  affects the activity of dopaminergic neurotransmitters, potentially leading to neurodegenerative disorders and mental issues, including anxiety, depression, language, and cognitive impairment [5–7]. In this context, a few fluorescent methods were developed for  $\text{Cu}^{2+}$  quantitative analysis in urine [8–14]. In this study, for the first time, the fluorescent properties of a novel fluorophore derived from serotonin (SE) self-oxidation and polymerization were exploited for sensitive  $\text{Cu}^{2+}$  detection in human urine without matrix pretreatment. SE is a neurotransmitter involved in multiple important physiological processes, such as memory, learning, anxiety, depression, cognition, vomiting, and vasoconstriction [15]. Very few studies describe the formation of SE oligomers [16–19], including polyserotonin (PSE) obtained using horseradish peroxidase (HRP) [19], and serotonin-based nanoparticles (PSE-NPs) [16,17] as multifunctional material for free radical scavenging, bioelectrical, and biomedical applications. In this paper, the highly emitting SE-derivative fluorophore (SEDF) was obtained by heating the SE monomer at an alkaline pH (Scheme 1a). SEDF was characterized by means of UV-Vis spectroscopy and mass spectrometry. The fluorescent properties of SEDF were outstanding when compared with the

fluorescent properties of polymers obtained using other endogenous neurotransmitters, i.e., polydopamine (PDA) and polynorepinephrine (PNE) [20,21]. The analytical performances of the fluorescence detection strategy were firstly evaluated by determining the  $\text{Cu}^{2+}$  in buffer and in artificial urine. Then, based on these results, we proceeded to determine the  $\text{Cu}^{2+}$  concentration in human urine samples (Scheme 1b) observing the reference values sufficient to detect the early stage of diseases associated with  $\text{Cu}^{2+}$  accumulation, such as chronic liver disease, acute hepatitis, and, primarily, Wilson's disease (WD), a rare inherited disorder that can lead to excess storage of copper in the liver, brain, and other organs [22,23]. Patients who suffer from WD have high urinary copper values between ca. 200 and 400  $\mu\text{g}$  per day [24,25]. Values of  $\text{Cu}^{2+}$  higher than 100  $\mu\text{g}$  per day are strongly indicative of this disease [23]. Common diagnostic assays for WD are based on the ceruloplasmin (Cp) concentration and on hepatic and urinary  $\text{Cu}^{2+}$  detection [23,26]. However, the Cp test is inaccurate for the estimation of free  $\text{Cu}^{2+}$ , whereas the evaluation of hepatic copper requires an invasive procedure and, often, the heterogeneous  $\text{Cu}^{2+}$  distribution within the liver leads to false negative results. Differently, the experimental procedure here developed for copper estimation would be noninvasive, fast, very simple, green, and low cost if compared to the reference instrumental approach for copper quantification in urine samples, such as inductively coupled plasma mass spectrometry (ICP-MS) [27], here used to validate the fluorescence method. This work aims to propose a new diagnostic tool for copper-dependent diseases, representing, to the best of our knowledge, the first example of copper ions detection exploiting the fluorescence quenching of a biopolymer.



**Scheme 1.** (a) Putative SEDF structure obtained by SE monomer polymerization upon linkage through the benzene ring after 2 h at 60 °C in 10 mM TRIS buffer pH 9; (b)  $\text{Cu}^{2+}$  detection in a 96-well microplate by reading the SEDF fluorescence quenching upon a  $[\text{Cu}^{2+}]$  increase in urine.

## 2. Materials and Methods

### 2.1. Chemicals

Serotonin ( $\text{C}_{10}\text{H}_{12}\text{N}_2\text{O}$ , 98% pure), tris(hydroxymethyl)aminomethane ( $\text{C}_4\text{H}_{11}\text{NO}_3$ , 99% pure), sodium hydroxide (NaOH,  $\geq 99\%$  pure), hydrochloric acid (HCl, 37% w/w,  $\geq 99\%$  pure), sodium chloride (NaCl,  $\geq 99\%$  pure), potassium chloride (KCl,  $\geq 99\%$  pure), lithium chloride (LiCl, 99% pure), and magnesium chloride ( $\text{MgCl}_2$ , 98% pure) were obtained from Thermo Fisher Scientific (Parma, Italy). Barium chloride ( $\text{BaCl}_2$ ,  $\geq 99\%$  pure), copper sulfate ( $\text{CuSO}_4$ ,  $\geq 99\%$  pure), bismuth (III) nitrate ( $\text{Bi}(\text{NO}_3)_3 \cdot 5\text{H}_2\text{O}$ , 98% pure), aluminum chloride ( $\text{AlCl}_3$ , 98% pure), zinc (II) sulphate ( $\text{ZnSO}_4 \cdot 7\text{H}_2\text{O}$ , 98% pure), cadmium (II) sulfate ( $\text{CdSO}_4 \cdot 8\text{H}_2\text{O}$ ,  $\geq 99\%$  pure), mercury (II) chloride ( $\text{HgCl}_2$ , 98% pure), silver chloride (AgCl, 99% pure), gold (III) chloride ( $\text{HAuCl}_4 \cdot 3\text{H}_2\text{O}$ , 99% pure), nickel (II) chloride ( $\text{NiCl}_2 \cdot 6\text{H}_2\text{O}$ , 99% pure), chloroplatinic acid solution ( $\text{H}_2\text{PtCl}_6$ , 99% pure), palladium (II) oxide (PdO, 99% pure), iron (III) chloride ( $\text{FeCl}_3 \times 6\text{H}_2\text{O}$ , 97% pure), potassium permanganate ( $\text{KMnO}_4$ , 98% pure), potassium chromate ( $\text{K}_2\text{Cr}_2\text{O}_7$ ,  $\geq 99\%$  pure), cobalt (II) chloride ( $\text{CoCl}_2 \cdot 6\text{H}_2\text{O}$ , 98% pure), ruthenium (IV) oxide ( $\text{RuO}_2$ ,  $\geq 99\%$  pure), acetonitrile

(C<sub>2</sub>H<sub>3</sub>N, ≥99% pure), DHB (2,5-dihydroxy benzoic acid, C<sub>7</sub>H<sub>6</sub>O<sub>4</sub>, 98% pure), glutamic acid (1 μM, C<sub>5</sub>H<sub>9</sub>NO<sub>4</sub>, 99% pure), glucose (2 μM, C<sub>6</sub>H<sub>12</sub>O<sub>6</sub>, 99% pure), ascorbic acid (2 μM, C<sub>6</sub>H<sub>8</sub>O<sub>6</sub>, ≥99% pure), hypoxanthine (9 μM, C<sub>5</sub>H<sub>4</sub>N<sub>4</sub>O, ≥99% pure), uric acid (4.5 μM, C<sub>5</sub>H<sub>4</sub>N<sub>4</sub>O<sub>3</sub>, ≥99% pure), creatinine (4 μM, C<sub>4</sub>H<sub>7</sub>N<sub>3</sub>O, ≥99% pure), urea (0.5 M, CH<sub>4</sub>N<sub>2</sub>O, ≥99% pure), sodium citrate (2 μM, Na<sub>3</sub>C<sub>6</sub>H<sub>5</sub>O<sub>7</sub>, ≥99% pure), trifluoroacetic acid (TFA, C<sub>2</sub>HF<sub>3</sub>O<sub>2</sub>, 98% pure), quinine sulfate (C<sub>20</sub>H<sub>26</sub>N<sub>2</sub>O<sub>6</sub>S, 99% pure, C<sub>40</sub>H<sub>50</sub>N<sub>4</sub>O<sub>8</sub>S), sulfuric acid (H<sub>2</sub>SO<sub>4</sub> ≥ 98% pure), 1-butanol (C<sub>4</sub>H<sub>10</sub>, HPLC purity reagent grade), water (H<sub>2</sub>O, HPLC purity reagent grade), Triton™ X100 (C<sub>14</sub>H<sub>22</sub>O(C<sub>2</sub>H<sub>4</sub>O)<sub>n</sub>, 98% purity reagent grade BioXtra), and tetramethylammonium hydroxide solution (TMAH, 25 wt% in H<sub>2</sub>O, 99% pure) were purchased from Merck (Milan, Italy). The artificial urine (AU) was from LCTech GmbH (Obertaufkirchen, Germany).

Human urine samples were collected from those destined for destruction at the Clinical Pathology Laboratory of the University Hospital in Pisa. Spiked samples were obtained and tested. Fluorescence measurements and ICP-MS experiments on the urine samples were performed in the Clinical Pathology Laboratory of the University Hospital in Pisa.

## 2.2. Instrumentation

The temperature-controlled synthesis reaction of SEDF was performed using a Thermomixer comfort (Eppendorf, VWR International, Milan, Italy). The fluorescence experiments were performed with fluorimeter FP-6500 (Jasco, Easton, PA, USA) using an excitation and emission wavelength of  $\lambda_{\text{ex}} = 350$  nm and  $\lambda_{\text{em}} = 450$  nm, respectively (emission bandwidth: 10 nm; excitation bandwidth: 5 nm; data pitch: 1 nm; scanning speed: 100 nm min<sup>-1</sup>; sensitivity: low) and microplate readers Fluoroskan Ascent (Thermo Fisher Scientific, Milan, Italy) by selecting as filter pairs  $\lambda_{\text{ex}} = 390$  nm and  $\lambda_{\text{em}} = 460$  nm, corresponding to the excitation and emission wavelengths, respectively. The absorbance measurements were obtained using a SPECTROstar Nano UV-Visible Spectrophotometer (Ortenberg, Germany) in 1.0 cm quartz cells at 20 °C. The mass spectrometry measurements, acquired in the positive-ion mode, were performed with a MALDI-TOF/TOF Ultraflex III (Bruker Daltonics, Milan, Italy) (matrix-assisted laser desorption/ionization time-of-flight mass spectrometry) by mixing the samples in a 1:1 ratio with 20 ng μL<sup>-1</sup> DHB (2,5-dihydroxy benzoic acid) as matrix dissolved in 70% of acetonitrile, 25% trifluoroacetic acid, and 5% ethanol. The mass spectra were acquired in the positive-ion mode.

## 2.3. Assay Protocol

### 2.3.1. Synthesis of Serotonin-Derived Fluorophore

A total of 2 g L<sup>-1</sup> of serotonin solution was dissolved in a 10 mM TRIS buffer pH 9.00 and heated at 60 °C for 2 h. Subsequently, the sample was left for 10 min at room temperature, then centrifuged 2 times for 10 min at 10,000 rpm. Finally, the supernatant was collected and stored at 4 °C after the addition of 5 mM HCl.

### 2.3.2. Quantum Yield Calculation

The fluorescence quantum yield ( $Q$ ) of the SEDF was estimated using quinine sulfate dissolved in 0.1 M H<sub>2</sub>SO<sub>4</sub> as the fluorescence reference standard of the known quantum yield ( $Q_R$ ), as reported by Lakowicz [28]. The quantum yield of the SEDF was calculated using the following equation:

$$Q = Q_R \times I/I_R \times OD_R/OD \times n^2/n_R^2$$

where  $I$  is the integrated fluorescence intensity,  $OD$  is the optical density at the excitation wavelength, and  $n$  is the refractive index of the solvent. The subscript  $R$  indicates the same parameters for the reference fluorophore, in this case quinine sulfate. The absorbances at the wavelength of excitation ( $\lambda_{\text{ex}} = 350$  nm) were kept at  $A = 0.05$  to avoid the inner filter effect [28], thus ensuring a linear dependence of the fluorescence signals to the sample concentration.

### 2.3.3. Copper Determination via the Fluorescence Quenching-Based Method

Stock  $\text{Cu}^{2+}$  solutions were prepared in 10 mM Tris pH 9.00 and in artificial urine. The different volumes of copper solution were mixed with solutions of previously synthesized SEDF (see above), immediately recording the fluorescence signal. The decrease in the fluorescence in dependence on the copper concentration was expressed as  $F_0/F$ , where  $F_0$  is the fluorescence of the SEDF without any metal addition, and  $F$  is the fluorescence recorded after the copper addition in buffer, artificial urine, and real urine samples. All measurements were performed at 25 °C in quadruplicates, at least. The limit of detection (LOD) and limit of quantification (LOQ) were calculated by applying the following equations:  $\text{LOD} = 3 \times \text{SD}_{\text{blank}}/\text{slope}$  and  $\text{LOQ} = 10 \times \text{SD}_{\text{blank}}/\text{slope}$ , where the standard deviation of the blanks ( $\text{SD}_{\text{blank}}$ ) was divided by the slope of the relative calibration plots.

### 2.3.4. ICP-MS Measurements

The method here developed was validated using an Agilent Technologies 7900 ICP-MS (Santa Clara, CA, USA) equipped with an ASX-500 Series autosampler and a peristaltic pump for the sample injection. The analyses were performed with the following acquisitions parameters: carrier gas flow rate of 0.80 L  $\text{min}^{-1}$  (Ar), aerosol dilution flow rate of 0.50 L  $\text{min}^{-1}$  (Ar), plasma gas flow rate of 15 L  $\text{min}^{-1}$  (Ar), collision gas flow rate of  $4.3 \times 10^{-3}$  L  $\text{min}^{-1}$  (He), RF power of 1550 W, stabilization time of 20 s, peak pattern of 3 point, 3 replicates, 100 sweeps per replicate, and a peristaltic pump speed of 0.1 rps. The system control and data acquisition and processing were carried out using the ICP-MS MassHunter Workstation<sup>®</sup> software, version 5.1. For the pre-analytical procedure, the Agilent environmental calibration standard mix, including copper ( $^{63}\text{Cu}$ ) at a concentration of 10,000  $\mu\text{g L}^{-1}$ , was diluted in deionized water to prepare an initial calibration curve ranging from 0 to 2500  $\mu\text{g L}^{-1}$ . The calibration points at 0, 0.1, 0.2, 0.5, 1, 2, 5, 10, 20, 50, 100, 200, and 250  $\mu\text{g L}^{-1}$  were obtained by dilution with water:1-butanol = 98.5:1.5 (*v/v*) added with Triton X100, 10  $\mu\text{L L}^{-1}$ , and Tetramethylammonium hydroxide solution (TMAH 25% in  $\text{H}_2\text{O}$ ), 100  $\mu\text{L L}^{-1}$ . Each calibration point was added with the appropriate amount of germanium ( $^{72}\text{Ge}$ ) as the internal standard. Two quality control points were added to attest the accuracy of the analysis. The urine samples, previously centrifuged at 1230 rpm for 15 min to remove the sediment, were analyzed after a dilution of 1:100 with water: 1-butanol solution with the appropriate amount of the internal standard.

## 3. Results and Discussion

### 3.1. Synthesis and Characterization of Serotonin-Derived Fluorophore (SEDF)

Recently, Jeon et al. reported the synthesis of insoluble polyserotonin nanoparticles from the self-oxidation of the SE monomer heated for 2 h at 60 °C in TRIS buffer at pH 9.00 [16]. Repeating the same procedure, we collected the supernatant solution instead of the precipitated nanoparticles, thus obtaining the serotonin-derived fluorophore (SEDF). The SEDF solution was brown in color with a  $\lambda_{\text{max}} = 470$  nm, indicative of a larger conjugated system with respect to the serotonin monomer showing the spectrum typical of a colorless indole derivative with maximum absorbance values at 280 nm and 300 nm (Figure 1a). Analogously, the fluorescence spectra of the SEDF showed a large emission band of approximately 450 nm, whereas in the same conditions the SE monomer was not fluorescent (Figure 1b).

Previous works refer to an SE dimer [29,30], while others describe an oligomer obtained through the electrochemical oxidation of serotonin [31–33]. To better understand the nature of the serotonin derivative obtained here, we performed mass spectrometry experiments by MALDI-TOF/TOF instrumentation. The peaks highlighted in Figure 2 ( $m/z$  176.689, 350.978, 502.098, and 672.180) are compatible with monomeric, dimeric, trimeric, and tetrameric structures, possibly obtained upon the linkage through the benzene ring (Scheme 1) [19]. However, the determination of the SEDF structure is out of the scope of this study and requires a much deeper analysis.

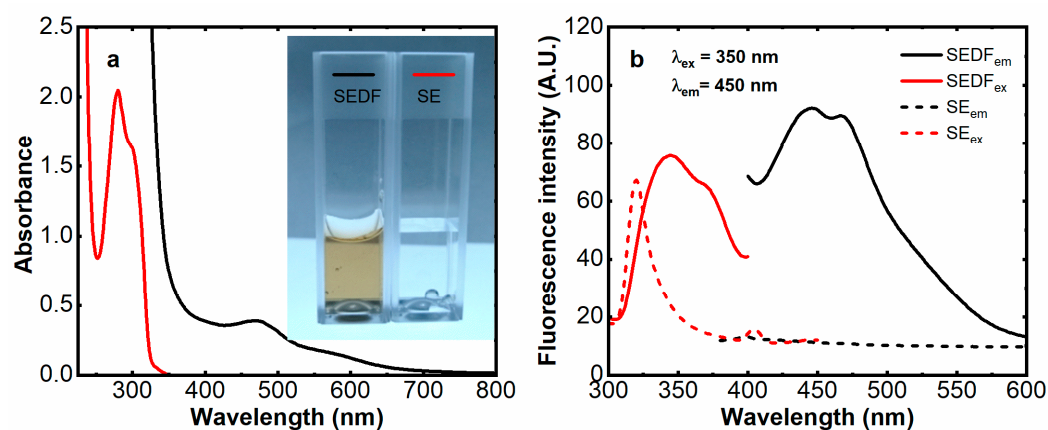


**Figure 1.** (a) UV-Vis spectra of the SE monomer (red line, right cuvette) and synthetic SEDF (black line, left cuvette) in 10 mM TRIS pH 9.00; (b) fluorescence excitation (red,  $\lambda_{em} = 450$  nm) and emission (black,  $\lambda_{ex} = 350$  nm) spectra of serotonin-derivative fluorophore (SEDF, thick line) and serotonin (SE, dashed line).

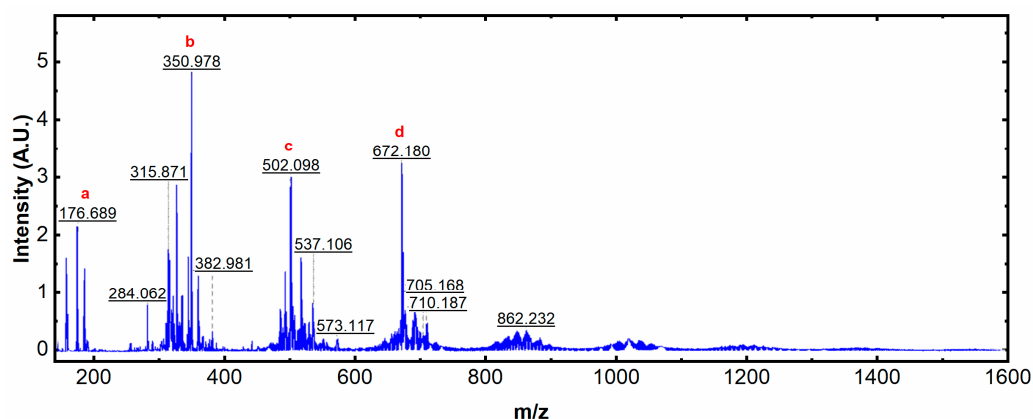


**Figure 2.** MALDI-TOF/TOF mass spectrum of the SE-derivative fluorophore (SEDF) obtained by heating  $2 \text{ g L}^{-1}$  serotonin at  $60^\circ \text{C}$  for 2 h in 10 mM TRIS at pH 9.00. The  $m/z$  values compatible with SE monomer (a), dimer (b), trimer (c), and tetramer (d) molecules are reported.

The influence of the synthetic parameters, such as pH, reaction time, and starting monomer concentration, on the fluorescent properties of the SEDF were tested (Figure 3) and, notably, the best fluorescence performances of the supernatant coincide with the best conditions for the size-controlled synthesis of polyserotonin nanoparticles [16].

In detail, the influence of the pH on the fluorescence of the SEDF was evaluated between 2.00 and 12.00. The solutions of the SEDF when excited at 350 nm showed emission spectra with a  $\lambda_{max}$  of approximately 400 nm at pH 2.00–4.00, 425 nm at pH 6.00–7.00, and 450–475 nm at pH 8.00–12.00 (Figure 3a,b). The intensity of the fluorescence emission was strongly reduced at a pH below 6.00 or above 11.00. Moreover, highly basic conditions led to heterogeneous mixtures with large scattering phenomena (data not shown). As shown in Figure 3b, the buffer at pH 9.00 resulted in the best fluorescence reproducibility with good fluorescence intensity, and this condition was used for the subsequent studies.

The influence of the temperature on the fluorescence of the SEDF at pH 9.00 for 2 h was evaluated between  $40^\circ \text{C}$  and  $90^\circ \text{C}$  (Figure 3c,d). The fluorescence emission of the SEDF increased with the temperature, and  $60^\circ \text{C}$  resulted in the temperature of choice, representing a good compromise in terms of the signal intensity and reproducibility (Figure 3d).

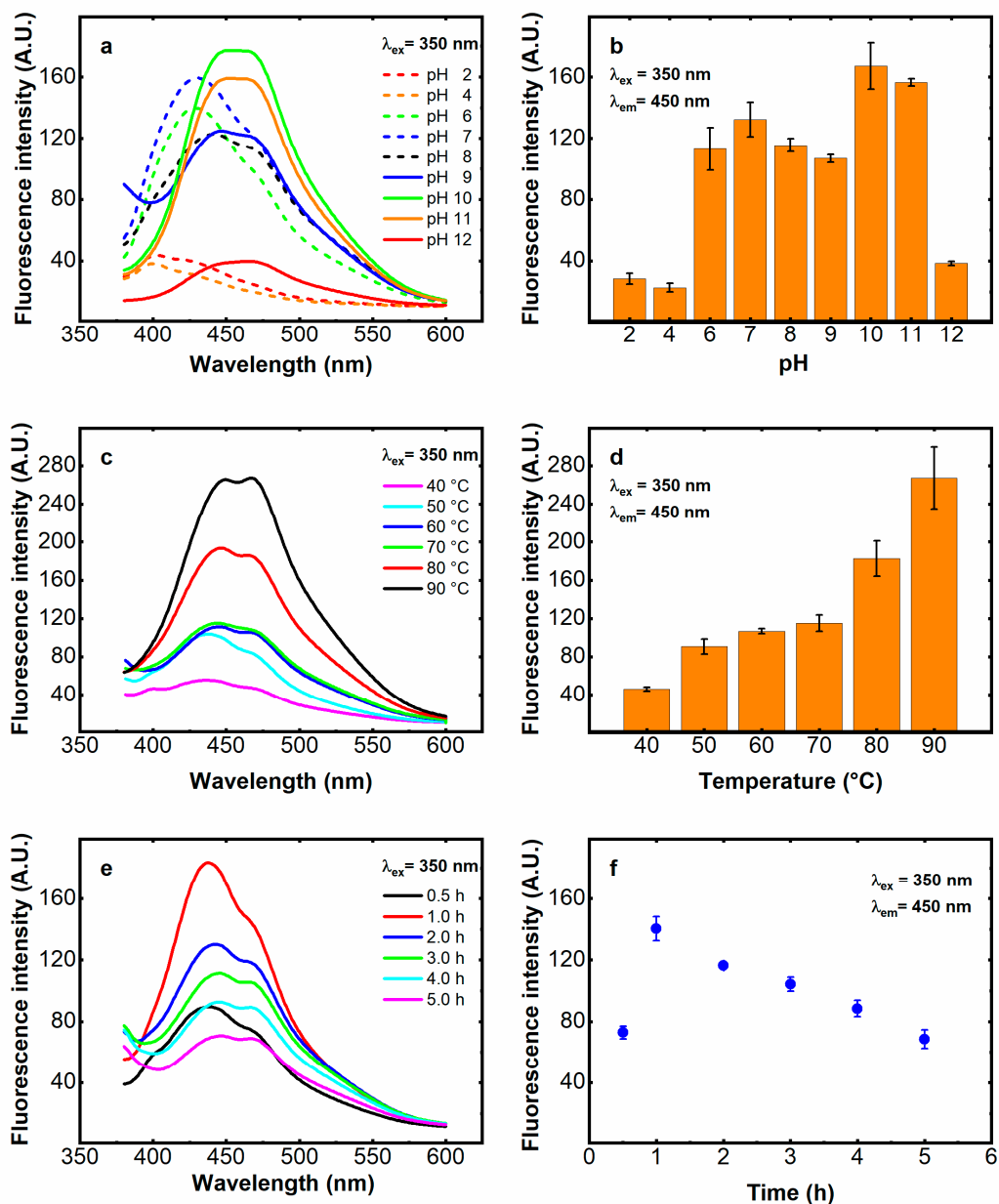


**Figure 3.** Fluorescence emission ( $\lambda_{\text{ex}} = 350 \text{ nm}$ ,  $\lambda_{\text{em}} = 450 \text{ nm}$ ) of serotonin-derivative fluorophore (SEDF) obtained by heating  $2.0 \text{ g L}^{-1}$  SE monomer. The influence of pH 2–12 (a,b), temperature  $40 \text{ }^{\circ}\text{C}$ – $90 \text{ }^{\circ}\text{C}$  (c,d), and reaction time 0.5–5 h (e,f) on the fluorescence emission spectra (left) and intensity at 450 nm (right). The error bars represent the standard deviation ( $n = 4$ ).

The influence of the reaction time on the fluorescence of the SEDF was evaluated between 30 min and 5 h at pH 9.00 and  $60 \text{ }^{\circ}\text{C}$ . The fluorescent spectrum of the SEDF was already visible after 30 min of reaction, reaching the maximum intensity after 1 h (Figure 3e,f). However, the best reproducibility was achieved after 2 h of reaction (Figure 3f).

Finally, the influence of SE monomer concentration on the fluorescence of SEDF after 2 h at pH 9.00 and  $60 \text{ }^{\circ}\text{C}$  (Figure 4a,b) was investigated. The largest fluorescence increase was obtained for SE up to  $0.5 \text{ g L}^{-1}$ , reaching a plateau at  $2 \text{ g L}^{-1}$  SE, which was fixed as the monomer concentration for the following experiments. The synthetic product was stabilized by adding 5 mM of HCl that stopped the oxidation process. The fluorescence intensity in buffer was stable up to 4 h, decreasing to 75% of the starting value after one month (Figure S1).

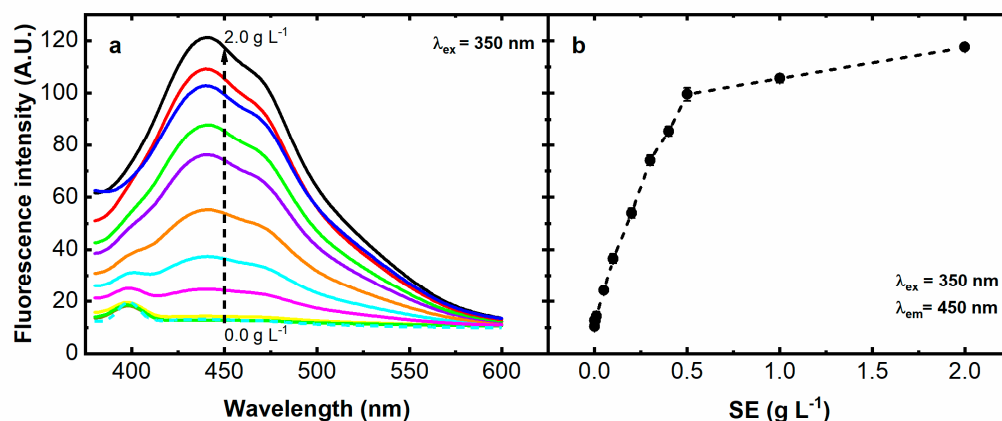


**Figure 4.** Influence of the serotonin monomer concentrations (0, 0.001, 0.005, 0.010, 0.050, 0.100, 0.200, 0.300, 0.400, 0.500, 1.000, and 2.000 g L<sup>-1</sup>) on the emission signal of the serotonin–derivative fluorophore synthesized after 2 h at 60 °C in alkaline conditions (pH 9.00). The fluorescence emission spectra upon excitation at 350 nm (a) and corresponding fluorescence emission intensity at 450 nm (b). The error bars represent the standard deviation (n = 4).

The fluorescence quantum yield (Q) of the SEDF was estimated in water, as reported in the assay protocol, and the obtained value of 0.025 was higher than the Q reported for the PSE obtained enzymatically (0.017) [19] and here calculated also for the PDA (0.019) and PNE (0.008), indicating the good fluorescent properties of such conjugated serotonin.

### 3.2. SEDF Fluorescence Quenching by Metal Ions

The effect of several solutions (0.5 mM) of alkaline, alkaline earth (Figure 5a), and transition metals (Figure 5b,c) on the SEDF fluorescence was evaluated, and it was found that only the latter quenched the fluorescence of the SEDF, in particular, Au<sup>3+</sup>, Cr<sub>2</sub>O<sub>7</sub><sup>2-</sup>, Fe<sup>3+</sup>, and Cu<sup>2+</sup> species (Figure 5c), which is in agreement with literature that reports on the fluorescence quenching of indole derivatives by copper ions and a few other metals [28,34,35]. The Fe<sup>3+</sup> exhibited a prominent fluorescence quenching, as previously observed for the fluorescent derivatives of dopamine used to quantify iron [36,37]. The fluorescence quenching was also large for Au<sup>3+</sup> and Cr<sub>2</sub>O<sub>7</sub><sup>2-</sup> ions but associated with low data reproducibility, which is also due to the formation of gold nanoparticles. Based on these results, and considering that, to the best of our knowledge, there are no studies on copper ion detection exploiting the fluorescence quenching of a polymer derived by an endogenous molecule, such as SEDF, we decided to apply this method to real urine samples, where the presence of large amounts of copper ions would be indicative of a pathological condition (see below), whereas the concomitant presence of the other quenching ions, in particular Au<sup>3+</sup> and Cr<sub>2</sub>O<sub>7</sub><sup>2-</sup>, is insignificant in urine [38,39], and the urinary level of iron in healthy people (0.2 mg L<sup>-1</sup>, 0.003 mM) is approximately two orders of magnitude below the concentration of Fe<sup>3+</sup> here tested (0.5 mM), and one order of magnitude below the minimum amount of Cu<sup>2+</sup> here spiked in urine (0.05 mM, vide infra). However, there is also the possible interference of larger urinary levels, as a consequence of other iron-overload diseases, which could be simply minimized by using the proper sequestering buffer, as already reported [40,41]. Moreover, we also evaluated the interference of the main organic compounds in urine on SEDF fluorescence quenching. As shown in Figure 5d, urea, uric acid, creatinine, and citrate, in the physiological concentration ranges [42], did not lead to a fluorescence quenching. This was also true for glucose, hypoxanthine, glutamic acid, and ascorbic acid at the concentration that determines the pathological state. Accordingly, we proceeded to determine the Cu<sup>2+</sup> concentration in buffer solution, artificial urine, and human urine samples.

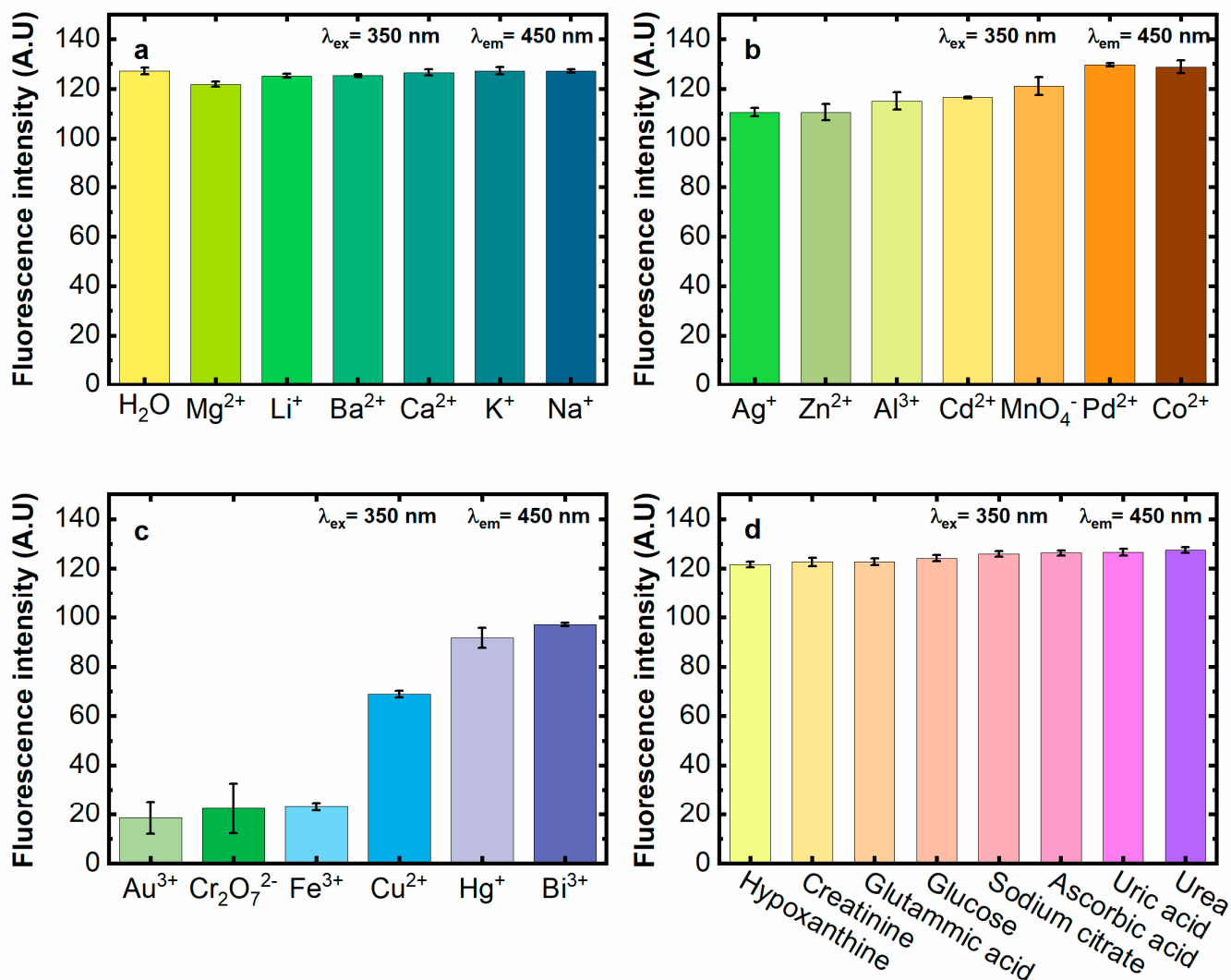


**Figure 5.** Fluorescence of the SEDF in 10 mM TRIS at pH 9.00 after the addition of 0.5 mM alkaline and alkaline earth metals (a), transition metals (b,c), and organic compounds occurring in urine (d). The error bars represent the standard deviation ( $n = 4$ ).

### 3.3. Copper Quantification via Quenching-Based Bioanalytical Assay

The SEDF fluorescence spectra and dose-response plots in the buffer and in artificial urine (AU) samples are reported in Figure 6. The fluorescence signal was reported as  $F_0/F$ , where  $F_0$  is the fluorescence intensity of the SEDF, and  $F$  is the emission signal of the SEDF after the copper addition. The fluorescence intensity at 450 nm after the  $\text{Cu}^{2+}$  addition was plotted versus the  $\text{Cu}^{2+}$  concentration in the range of 0.05–0.5 mM, following a linear trend with remarkable analytical performance (Table S1), both in the buffer and in AU samples, as confirmed by the correlation coefficient  $R^2 = 0.990$  for both and by the linear fitting equations  $F_0/F = 4.68 \times [\text{Cu}^{2+}] + 0.87$  used for the  $\text{Cu}^{2+}$  detection in buffer and  $F_0/F = 3.38 \times [\text{Cu}^{2+}] + 0.93$  for AU. The excellent assay reproducibility was highlighted by the low variability ( $\text{CV}_{\text{av}}\% = 4\%$  for buffer and 3% for AU), with an LOD of  $16 \pm 1 \mu\text{g L}^{-1}$  and an LOQ of  $54 \pm 2 \mu\text{g L}^{-1}$  in buffer solution and an LOD of  $22 \pm 1 \mu\text{g L}^{-1}$  and LOQ of  $75 \pm 3 \mu\text{g L}^{-1}$  in AU (Table S1). Notably, these concentrations are below the values of copper associated to the pathological state of Wilson's diseases [24,25], stimulating the application of this assay to human urine samples.



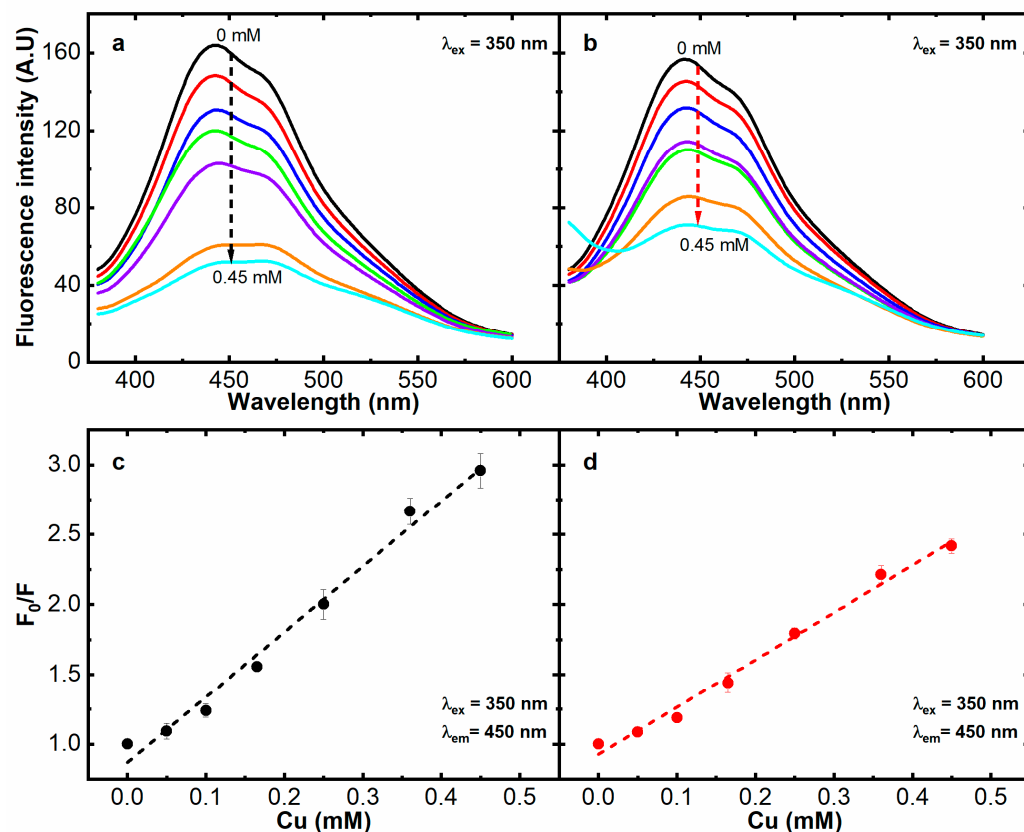


**Figure 6.** Fluorescence spectra and the relative calibration plots of the SEDF after copper ion addition in buffer (a,c) and in artificial urine samples (b,d). The fluorescence was recorded at 450 nm ( $\lambda_{ex} = 350$  nm) and reported as a  $F_0/F$  versus  $\text{Cu}^{2+}$  concentration (0, 0.010, 0.050, 0.100, 0.165, 0.250, 0.350, and 0.450 mM), where  $F_0$  and  $F$  represent the fluorescence intensity of the SEDF before and after the copper addition, respectively. The error bars represent the standard deviation ( $n = 4$ ). The analytical parameters are reported in Table S1.

### 3.4. Copper Detection in Human Urine Samples

With the aim to design a bioassay for the urinary  $\text{Cu}^{2+}$  quantification for clinical purposes, we transferred our experiments in ELISA-type 96-well microplates, allowing for the immediate and simultaneous analysis of several human urine samples and reducing the turnaround time for the analysis. Another advantage offered by the method here developed is the direct analysis of the urine samples without any pretreatment.

The urine samples were preliminarily assayed by ICP-MS to determine the starting copper physiological concentration, resulting in the nM range (Table S3). Among them, the urine sample n. 3 was selected to be used as a calibrator in the real matrix by  $\text{Cu}^{2+}$  standard additions (red line in Figure 7), since its  $\text{Cu}^{2+}$  level represents a mean value within the series. The  $\text{CV}_{av}\%$  (1%) and the slope reported in Table S3 highlight the high reproducibility and sensitivity of the method, even in the complex real matrix, with an LOD and LOQ of  $59 \pm 3 \mu\text{g L}^{-1}$  and  $97 \pm 11 \mu\text{g L}^{-1}$ , respectively.

Subsequently, 100  $\mu\text{L}$  of each urine sample was spiked with different known  $\text{Cu}^{2+}$  concentrations (0.05 mM; 0.20 mM, and 0.40 mM, see Table 1) and added to 1800  $\mu\text{L}$  of the SEDF solution. These spiked samples were analyzed in parallel by fluorescence and ICP-MS (Table 1 and Figure 7).

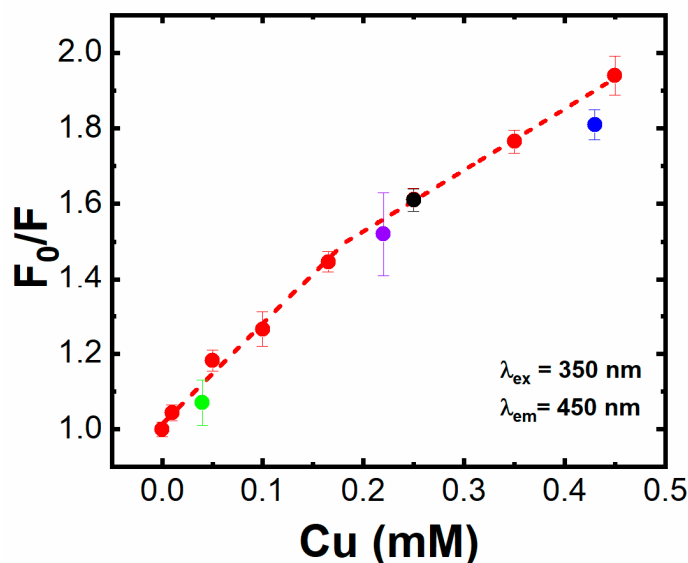


**Figure 7.** Calibration of  $\text{Cu}^{2+}$  in human urine (sample 3, red dots and fitting) and its quantification in the four urine samples, indicated by the different colors (1—green, 2—violet, 3—black, and 4—blue). The fluorescent signal is reported as  $F_0/F$  at  $\lambda_{\text{em}} = 450 \text{ nm}$  ( $\lambda_{\text{ex}} = 350 \text{ nm}$ ) versus the  $\text{Cu}^{2+}$  concentration, where  $F_0$  and  $F$  represent the fluorescence intensity of the SEDF before and after the copper addition, respectively. The error bars represent the standard deviation ( $n = 4$ ). The analytical parameters of the calibration are reported in Table S2 and were obtained using the piecewise linear fitting implemented in the OriginPro software, version 2022. OriginLab Corporation, Northampton, MA, USA.

**Table 1.**  $\text{Cu}^{2+}$  concentrations in the reinforced urine samples (Figure 7).

#	<sup>1</sup> [ $\text{Cu}^{2+}$ ]	$F_0/F$	<sup>2</sup> [ $\text{Cu}^{2+}$ ]	<sup>3</sup> [ $\text{Cu}^{2+}$ ]	<sup>4</sup> Recovery (%)
1	0.05 mM	$1.07 \pm 0.06$	$0.04 \text{ mM} \pm 0.02$	0.03 mM	133%
2	0.20 mM	$1.52 \pm 0.11$	$0.22 \text{ mM} \pm 0.01$	0.21 mM	105%
3	0.20 mM	$1.61 \pm 0.03$	$0.25 \text{ mM} \pm 0.01$	0.22 mM	114%
4	0.40 mM	$1.81 \pm 0.04$	$0.43 \text{ mM} \pm 0.01$	0.49 mM	88%

<sup>1</sup> Spiked; <sup>2</sup> quenching-based method; <sup>3</sup> ICP-MS; <sup>4</sup>  $100 \times [\text{Cu}^{2+}]_{\text{Quenching}} / [\text{Cu}^{2+}]_{\text{ICP-MS}}$ .

Despite the complexity and the variability of the analyzed urine samples, the results clearly highlight the very good accuracy of the assay with respect to the calibrator, even if the urine sample n. 2 showed a slightly higher variability, likely due to the marked turbidity and the darker color of the sample. This allows us to foresee the realistic applicability of the method as a diagnostic tool, covering a broad range of  $\text{Cu}^{2+}$  concentrations expected in this type of patient.

### 3.5. Assay Performance Compared to Other Fluorescence-Based Method for Copper Detection

The quenching-based assay here designed was finally compared to the recently developed fluorescence-based methods for  $\text{Cu}^{2+}$  detection in urine [8–11] (Table S4), i.e., carbon dots (CDs) combined with covalent organic frameworks (COFs), chitosan/L-histidine-stabilized silicon nanoparticles (CS/L-His-SiNPs), nitrogen-doped quantum carbon dots (ND-CQDs), and blue CDs (bCDs) combined with green quantum dots (gQDs). These methods offer better LODs values [8,9] (except in Li et al. and Zhang et al., in which the LOD values were not calculated for human urine samples [10,11]). However, these nanostructures require long and laborious synthetic procedures. Contrarily, herein, SEDF was rapidly (2 h) synthesized and, for the first time, this novel biomaterial was applied for diagnostic purposes.

#### 4. Conclusions

In this study, the fluorescent properties of a serotonin-derived fluorophore were successfully exploited for urinary  $\text{Cu}^{2+}$  determination via a quenching-based bioanalytical method. To the best of our knowledge, this is the first example of a quenching-based assay that exploits the fluorescent properties of a polymer derived by an endogenous molecule. The SEDF's spectroscopic features were deeply investigated, and different techniques were applied to characterize this novel material, including mass spectrometry confirming its oligomeric state. The experimental conditions were optimized to obtain the highest emission signal and to improve the assay sensitivity and reproducibility. The whole protocol was performed within 2 h in line with clinical requirements. The  $\text{Cu}^{2+}$  ions were firstly quantified in buffer and in artificial urine obtaining very low variability, high sensitivity, and low LOD and LOQ values. Then, the assay was applied to estimate the  $\text{Cu}^{2+}$  concentration in human urine samples from volunteers and, finally, validated by ICP-MS obtaining very good recovery values and excellent analytical performances in a real matrix, namely, a  $\text{CV}_{\text{av}}\%$  of 1%, an LOD of  $59 \pm 3 \mu\text{g L}^{-1}$ , and an LOQ of  $97 \pm 11 \mu\text{g L}^{-1}$ . These values are below the concentrations of urinary  $\text{Cu}^{2+}$  that, for example, determine the pathological state of Wilson's disease ( $60\text{--}240 \mu\text{g L}^{-1}$ ), enabling the applicability of the method for  $\text{Cu}^{2+}$  measurement in routine clinical practice without the need of sample pretreatment.

**Supplementary Materials:** The following supporting information can be downloaded at: <https://www.mdpi.com/article/10.3390/s23063030/s1>, Figure S1: Fluorescence stability over time for serotonin-derivative fluorophore (SEDF); Table S1:  $\text{Cu}^{2+}$  detection in buffer and in AU. Data are from Figure 6; Table S2:  $\text{Cu}^{2+}$  quantification in human urine. Data are from Figure 7; Table S3: Physiological  $\text{Cu}^{2+}$  concentration of human urine samples; Table S4: Fluorescent-based assays for  $\text{Cu}^{2+}$  quantitative analysis in human urine samples.

**Author Contributions:** Conceptualization, M.L., S.S., P.P. and M.M.; investigation, M.L., S.S., L.C., A.B., A.S., P.P. and M.M.; writing—review and editing, M.L., S.S., L.C., A.B., A.S., P.P. and M.M. All authors have read and agreed to the published version of the manuscript.

**Funding:** The financial support provided by the MUR—Dipartimenti di Eccellenza 2023–2027 (DICUS 2.0) to the Department of Chemistry “Ugo Schiff” of the University of Florence is acknowledged.

**Institutional Review Board Statement:** The study was conducted in accordance with the Declaration of Helsinki and approved by the Institutional Ethics Committee of the Clinical Pathology Laboratory of the University Hospital in Pisa (CEAVNO, 13 February 2020).

**Informed Consent Statement:** Patient consent was waived because the samples consisted of sample residues, normally destined for destruction, used as a biological matrix to disperse the analyte. Furthermore, the residues were anonymized so that no clinical information could be traced back to the sample.

**Data Availability Statement:** Data available upon request.

**Conflicts of Interest:** The authors declare no conflict of interest.

#### References

1. Maung, M.T.; Carlson, A.; Olea-Flores, M.; Elkhadragey, L.; Schachtschneider, K.M.; Navarro-Tito, N.; Padilla-Benavides, T. The molecular and cellular basis of copper dysregulation and its relationship with human pathologies. *FASEB J.* **2021**, *35*, e21810. [[CrossRef](#)] [[PubMed](#)]
2. Tsang, T.; Davis, C.I.; Brady, D.C. Copper biology. *Curr. Biol.* **2021**, *31*, R421–R427. [[CrossRef](#)] [[PubMed](#)]
3. National Research Council (US). *Committee on Copper in Drinking Water*; National Academies Press (US): Washington, DC, USA, 2000. Available online: <https://www.ncbi.nlm.nih.gov/books/NBK225407/> (accessed on 1 March 2023).
4. Zuily, L.; Lahrach, N.; Fassler, R.; Genest, O.; Faller, P.; Sénèque, O.; Denis, Y.; Castanié-Cornet, M.P.; Genevaux, P.; Jakob, U.; et al. Copper Induces Protein Aggregation, a Toxic Process Compensated by Molecular Chaperones. *MBio* **2022**, *13*, e03251–21. [[CrossRef](#)] [[PubMed](#)]
5. Donnelly, P.S.; Xiao, Z.; Wedd, A.G. Copper and Alzheimer's disease. *Curr. Opin. Chem. Biol.* **2007**, *11*, 128–133. [[CrossRef](#)] [[PubMed](#)]

6. Davies, K.M.; Mercer, J.F.B.; Chen, N.; Double, K.L. Copper dyshomeostasis in Parkinson's disease: Implications for pathogenesis and indications for novel therapeutics. *Clin. Sci.* **2016**, *130*, 565–574. [[CrossRef](#)]
7. Ni, M.; You, Y.; Chen, J.; Zhang, L. Copper in depressive disorder: A systematic review and meta-analysis of observational studies. *Psychiatry Res.* **2018**, *267*, 506–515. [[CrossRef](#)]
8. Arputharaj, E.; Singh, S.; Pasupuleti, R.R.; Dahms, H.U.; Huang, Y.L. Visible fluorescent sensing of Cu<sup>2+</sup> ions in urine by reusable chitosan/L-histidine-stabilized silicon nanoparticles integrated thin layer chromatography sheet. *Anal. Chim. Acta.* **2022**, *1231*, 340418. [[CrossRef](#)]
9. Ma, X.; Yang, Y.; Ma, R.; Zhang, Y.; Zou, X.; Zhu, S.; Ge, X.; Yuan, Y.; Zhang, W.; Zhu, G. Inorganic nanocrystal-dynamic porous polymer assemblies with effective energy transfer for sensitive diagnosis of urine copper. *Chem. Sci.* **2020**, *11*, 12187–12193. [[CrossRef](#)]
10. Zhao, L.; Li, H.; Xu, Y.; Liu, H.; Zhou, T.; Huang, N.; Li, Y.; Ding, L. Selective detection of copper ion in complex real samples based on nitrogen-doped carbon quantum dots. *Anal. Bioanal. Chem.* **2018**, *410*, 4301–4309. [[CrossRef](#)]
11. Cai, Y.; You, J.; You, Z.; Dong, F.; Du, S.; Zhang, L. Profuse color-evolution-based fluorescent test paper sensor for rapid and visual monitoring of endogenous Cu<sup>2+</sup> in human urine. *Biosens. Bioelectron.* **2018**, *99*, 332–337. [[CrossRef](#)]
12. Nsanamahoro, S.; Wang, W.F.; Zhang, Y.; Shi, Y.P.; Yang, J.L. Synthesis of orange-emissive silicon nanoparticles as “off-on” fluorescence probe for sensitive and selective detection of L-methionine and copper. *Talanta* **2021**, *231*, 122369. [[CrossRef](#)] [[PubMed](#)]
13. Zhang, W.J.; Liu, S.G.; Han, L.; Luo, H.Q.; Li, N.B. A ratiometric fluorescent and colorimetric dual-signal sensing platform based on N-doped carbon dots for selective and sensitive detection of copper(II) and pyrophosphate ion. *Sens. Actuators B Chem.* **2019**, *283*, 215–221. [[CrossRef](#)]
14. Yang, Y.; Chen, P.; Liu, Y.; Cai, Z.; Wang, X.; Me, Y.; Ding, X.; Lin, L.; Jiang, H.; Zhang, Z.; et al. A colorimetric indicator-displacement assay based on stable Cu<sup>2+</sup> selective carbon dots for fluorescence turn-on detection of pyrophosphate anions in urine. *Spectrochim. Acta Part A Mol. Biomol. Spectrosc.* **2021**, *251*, 119479. [[CrossRef](#)] [[PubMed](#)]
15. Mohammad-Zadeh, L.F.; Moses, L.; Gwaltney-Brant, S.M. Serotonin: A review. *J. Vet. Pharmacol. Ther.* **2008**, *31*, 187–199. [[CrossRef](#)]
16. Jeon, K.; Andoy, N.M.O.; Schmitt, C.W.; Xue, Y.; Barner, L.; Sullan, R.M.A. Size-controlled synthesis of bioinspired polyserotonin nanoparticles with free radical scavenging activity. *J. Mater. Chem. B* **2021**, *9*, 634–637. [[CrossRef](#)]
17. Nakatsuka, N.; Hasani-Sadrabadi, M.; Cheung, K.; Young, T.; Bahlakeh, G.; Moshaverinia, A.; Weiss, P.; Andrews, A. Polyserotonin Nanoparticles as Multifunctional Materials for Biomedical Applications. *ACS Nano* **2018**, *12*, 4761–4774. [[CrossRef](#)]
18. Ishino, K.; Nishitani, S.; Man, Y.; Saito, A.; Sakata, T. Surface Characteristics and Formation of Polyserotonin Thin Films for Bioelectrical and Biocompatible Interfaces. *ACS Appl. Mater. Interfaces* **2022**, *38*, 8633–8642. [[CrossRef](#)] [[PubMed](#)]
19. Kiratitanavit, W.; Bruno, F.F.; Xia, Z.; Yu, S.; Kumar, J.; Nagarajan, R. Biocatalytic synthesis of fluorescent conjugated polyserotonin. *J. Renew. Mater.* **2019**, *7*, 205–214. [[CrossRef](#)]
20. Farahmand Nejad, M.A.; Ghasemi, F.; Hormozi-Nezhad, M.R. A wide-color-varying ratiometric nanoprobe for detection of norepinephrine in urine samples. *Anal. Chim. Acta* **2018**, *1039*, 124–131. [[CrossRef](#)]
21. Koh, D.Y.; Kook, J.K.; Lee, S.W. Highly fluorescent oligodopamine (F-ODA) for accurate and sensitive detection of the neurotransmitter dopamine. *Anal. Biochem.* **2020**, *591*, 113571. [[CrossRef](#)]
22. Moini, M.; To, U.; Schilsky, M.L. Recent advances in Wilson disease. *Transl. Gastroenterol. Hepatol.* **2021**, *6*, 21. [[CrossRef](#)]
23. Brewer, G.J.; Gow, P.J.; Smallwood, R.A.; Angus, P.W.; Sewell, R.B.; Smith, A.L.; Wall, A.J. Diagnosis of Wilson's disease: An experience over three decades. *Gut* **2002**, *50*, 136. [[CrossRef](#)] [[PubMed](#)]
24. Walshe, J.M. The pattern of urinary copper excretion and its response to treatment in patients with Wilson's disease. *Qjm* **2011**, *104*, 775–778. [[CrossRef](#)] [[PubMed](#)]
25. Gray, L.W.; Peng, F.; Molloy, S.A.; Pendyala, V.S.; Muchenditsi, A.; Muzik, O.; Lee, J.; Kaplan, J.H.; Lutsenko, S. Urinary Copper Elevation in a Mouse Model of Wilson's Disease Is a Regulated Process to Specifically Decrease the Hepatic Copper Load. *PLoS ONE* **2012**, *7*, e38327. [[CrossRef](#)]
26. Woimant, F.; Djebrani-Oussedik, N.; Poujois, A. New tools for Wilson's disease diagnosis: Exchangeable copper fraction. *Ann. Transl. Med.* **2019**, *7*, S70. [[CrossRef](#)] [[PubMed](#)]
27. Robson, A.F.; Lockett, P.; Tetlow, L.; Chaloner, C. Evaluation of 24-h urine containers for urine copper measurement by inductively coupled plasma mass spectrometry. *Ann. Clin. Biochem.* **2020**, *57*, 246–248. [[CrossRef](#)]
28. Lakowicz, J.R. *Principles of Fluorescence Spectroscopy*, 3rd ed.; Springer: Boston, MA, USA, 2006; pp. 54–55. [[CrossRef](#)]
29. Heuther, G.; Reimer, A.; Schmidt, F.; Schuff-Werner, P.; Brudny, M.M. Oxidation of the indole nucleus of 5-hydroxytryptamine and formation of dimers in the presence of peroxidase and H<sub>2</sub>O<sub>2</sub>. *J. Neural Transm. Suppl.* **1990**, *32*, 249–257. [[CrossRef](#)]
30. Dai, Z.; Chauhan, S.; Green, T.K. Synthesis and enantioseparation of atropisomers of serotonin dimer. *Tetrahedron Lett.* **2015**, *56*, 4022–4024. [[CrossRef](#)]
31. Wrona, M.Z.; Dryhurst, G. Electrochemical oxidation of 5-hydroxytryptamine in aqueous solution at physiological pH. *Bioorg. Chem.* **1990**, *18*, 291–317. [[CrossRef](#)]
32. Wrona, M.Z.; Dryhurst, G. Oxidation Chemistry of 5-Hydroxytryptamine. 1. Mechanism and Products Formed at Micromolar Concentrations. *J. Org. Chem.* **1987**, *52*, 2817–2825. [[CrossRef](#)]

33. Jones, C.E.; Underwood, C.K.; Coulson, E.J.; Taylor, P.J. Copper induced oxidation of serotonin: Analysis of products and toxicity. *J. Neurochem.* **2007**, *102*, 1035–1043. [[CrossRef](#)]
34. Strambini, G.B.; Gabellieri, E. Quenching of indole luminescence by copper ions: A distance dependence study. *J. Phys. Chem.* **1991**, *95*, 4347–4352. [[CrossRef](#)]
35. Bu, J.; Duan, H.; Wang, X. Fluorescence sensors for Cu<sup>2+</sup> based on conjugated indole Schiff base. *Res. Chem. Intermed.* **2014**, *40*, 3119–3126. [[CrossRef](#)]
36. Lin, J.H.; Yu, C.J.; Yang, Y.C.; Tseng, W.L. Formation of fluorescent polydopamine dots from hydroxyl radical-induced degradation of polydopamine nanoparticles. *Phys. Chem. Chem. Phys.* **2015**, *17*, 15124–15130. [[CrossRef](#)]
37. An, T.; Lee, N.; Cho, H.J.; Kim, S.; Shin, D.S.; Lee, S.M. Ultra-selective detection of Fe<sup>2+</sup> ion by redox mechanism based on fluorescent polymerized dopamine derivatives. *RSC Adv.* **2017**, *7*, 30582–30587. [[CrossRef](#)]
38. García-Moreno, E.; Tomás, A.; Atrián-Blasco, E.; Gascón, S.; Romanos, E.; Rodríguez-Yoldi, J.M.; Cerrada, E.; Laguna, M. In vitro and in vivo evaluation of organometallic gold(I) derivatives as anticancer agents. *Dalt. Trans.* **2016**, *45*, 2462–2475. [[CrossRef](#)]
39. Zhou, Q.; Guo, W.; Jia, Y.; Xu, J. Comparison of chromium and iron distribution in serum and urine among healthy people and prediabetes and diabetes patients. *Biomed. Res. Int.* **2019**, *2019*, 3801639. [[CrossRef](#)]
40. Serrat, F.B. Colorimetric method for determination of chlorine with 3,3',5,5'-tetramethylbenzidine. *Talanta* **1994**, *41*, 2091–2094. [[CrossRef](#)]
41. Palladino, P.; Torrini, F.; Scarano, S.; Minunni, M. 3,3',5,5'-tetramethylbenzidine as multi-colorimetric indicator of chlorine in water in line with health guideline values. *Anal. Bioanal. Chem.* **2020**, *412*, 7861–7869. [[CrossRef](#)]
42. Sarigul, N.; Korkmaz, F.; Kurultak, İ. A New Artificial Urine Protocol to Better Imitate Human Urine. *Sci. Rep.* **2019**, *9*, 20159. [[CrossRef](#)]

**Disclaimer/Publisher's Note:** The statements, opinions and data contained in all publications are solely those of the individual author(s) and contributor(s) and not of MDPI and/or the editor(s). MDPI and/or the editor(s) disclaim responsibility for any injury to people or property resulting from any ideas, methods, instructions or products referred to in the content.